

Proposal to the ISOLDE and NTOF committee

Elastic scattering and reaction mechanisms in the collision ${}^8\text{B}+{}^{64}\text{Zn}$ around the Coulomb barrier.

A.Di Pietro¹, P.Figuera¹, M.Fisichella^{1,2}, M.Lattuada^{1,2}, M.Milin³, A.Musumarra¹², M.G.Pellegriti¹², V.Scuderi¹², D.Torresi¹², E.Strano¹², N.Soic⁴, M.Zadro⁴.

1)INFN-Laboratori Nazionali del Sud and Sezione di Catania, Italy

2) Universita' di Catania, Catania, Italy

3)Department of Physics Faculty of Science University of Zagreb, Zagreb, Croatia

4)Division of Experimental Physics Ruder Boskovic Institute, Zagreb, Croatia

Spokespersons: A.DiPietro, P.Figuera

Abstract

We propose to use a post-accelerated ${}^8\text{B}$ beam and a large solid angle detection setup, having good angular resolution, to study elastic scattering and direct reaction processes in the collision ${}^8\text{B}+{}^{64}\text{Zn}$. The aim of the experiment is to investigate on effects of the weakly bound ($S_p=138$ keV) proton halo on the reaction mechanisms around the Coulomb barrier. In order to perform this experiment the ${}^8\text{B}$ beam needs to be developed at ISOLDE.

1. Introduction: reaction mechanisms around the barrier with halo nuclei

The study of elastic scattering and reaction mechanisms in collisions induced by halo nuclei around the Coulomb barrier is a challenging problem in nuclear reaction studies. Scattering and reaction processes depend upon the projectile halo structure, as well as on the coupling to bound and unbound states of the halo nucleus and to other relevant reaction channels. In order to investigate on these effects high quality data are necessary; however, due to the quality of radioactive beams, these are not always available (see e.g. [1] for a review).

1.1 ${}^6\text{He}$ induced reactions

Since ${}^6\text{He}$ beams are available at different facilities with intensities up to 10^7 pps, in a wide range of energies, several experiments have been performed so far using mainly this two neutron halo nucleus, on different targets. A common feature observed in the ${}^6\text{He}$ induced elastic scattering is a reduction of the elastic cross section in the region of the Coulomb-nuclear interference peak [e.g. 2,3] often called in the literature Coulomb "rainbow" or Fresnel-diffraction [4]. For brevity, in the



following, we will refer to the Coulomb-nuclear interference peak as "rainbow". A consequence of the "rainbow" suppression, in collisions induced by the halo ${}^6\text{He}$ nucleus, is a much larger total-reaction cross-section than the one observed in reactions induced by the corresponding well bound ${}^4\text{He}$ isotope.

As an example, in our previous study of reaction mechanisms in the systems ${}^4,6\text{He}+{}^{64}\text{Zn}$ around the barrier [2] we found a total reaction cross section for ${}^6\text{He}$ case, two times larger than the one for ${}^4\text{He}$. A large yield of alpha particles due to transfer and breakup reactions, saturating up to 80% of the total reaction cross section, was also observed.

Similar results have been found also by other authors in different systems [e.g. 5,6]. It is indeed confirmed that total reaction cross sections in collisions induced by ${}^6\text{He}$ around and below the Coulomb barrier are much larger than the corresponding ones for ${}^4\text{He}$ and are dominated by direct reaction processes like transfer and breakup. The relative contribution of transfer and breakup has been clearly separated in the systems ${}^6\text{He}+{}^{209}\text{Bi}$ and ${}^6\text{He}+{}^{65}\text{Cu}$ showing that transfer is the most important contribution [7,8].

Different conclusions have been reached by different authors concerning the effect of the halo structure on the fusion cross sections around and below the barrier. For some systems like ${}^6\text{He}+{}^{64}\text{Zn}$ [2] or ${}^6\text{He}+{}^{238}\text{U}$ [6] no effect on fusions were evidenced whereas in other cases like ${}^6\text{He}+{}^{209}\text{Bi}$ [9] or ${}^6\text{He}+{}^{197}\text{Au}$ [10] an enhancement of the fusion cross section below the barrier was found. The study of the fusion reaction channel, however, is not a goal of the present proposal.

A common feature observed by different authors in fitting experimental elastic scattering angular distributions of collisions induced by ${}^6\text{He}$ halo nuclei via Optical Model is the need to use a large diffuseness of the imaginary part of the potential in order to take into account the diffuse structure of the ${}^6\text{He}$ halo and to reproduce the data [3,5,11]. Continuum Discretized Coupled Channel calculations (CDCC) of the ${}^6\text{He}$ elastic-scattering [12-15] on different targets have also been performed. In order to simplify the very complicated calculations for the three body (n-n-alpha) ${}^6\text{He}$ system, two body representations of ${}^6\text{He}$ are often considered, where ${}^6\text{He}$ is represented as an alpha- 2n system. Techniques to perform four-body (n-n-alpha + target) CDCC calculations have recently been developed [14,15] and good agreement with the data is obtained in some cases.

Due to the complexity of the ${}^6\text{He}$ structure, to test the theoretical models, it would be of great help the availability of detailed elastic-scattering data on other halo systems, such as ${}^{11}\text{Be}$, ${}^{11}\text{Li}$, or ${}^8\text{B}$. Moreover, coupling effects of break-up or transfer depend upon nuclear structure properties of projectile and/or target as well as break-up thresholds or beam energies. Therefore drawing general conclusions about channel coupling effects on a limited sets of reactions induced by ${}^6\text{He}$ could be misleading [e.g. 1,16].

1.2 ${}^{11}\text{Be}$ induced collisions

The only data published so far on reaction mechanisms study around the Coulomb barrier with neutron halo nuclei, different than ${}^6\text{He}$, concerns the system ${}^{11}\text{Be}+{}^{209}\text{Bi}$ [17,18]. The authors used a fragmentation beam degraded in energy selecting, via a tagging procedure, beam energy bins having a 2 MeV width. The quasi elastic cross-section, which included inelastic-scattering to the first excited state of ${}^{11}\text{Be}$ and target excited states up to 2.6 MeV, was measured.

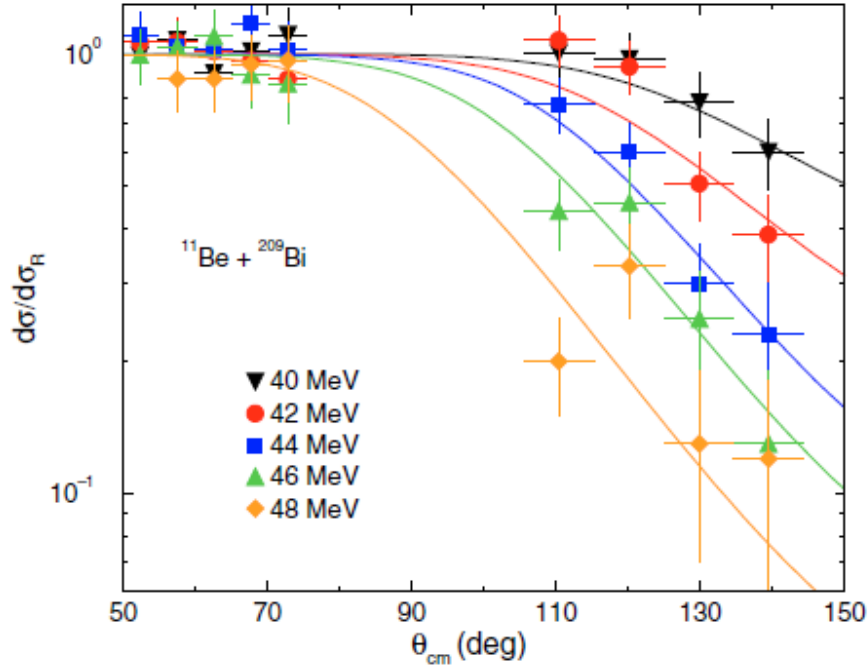


Figure 1 Quasi elastic scattering angular distributions measured in [17] for the system $^{11}\text{Be}+^{209}\text{Bi}$ using a ^{11}Be beam produced in fragmentation reactions, separated in flight and degraded in energy.

The total reaction cross-sections extracted by the analysis of the elastic angular distributions shown in figure 1 were found to be similar to the ones of $^9\text{Be}+^{209}\text{Bi}$, measured by the same group. Since the fusion cross sections for the $^{9,11}\text{Be}+^{209}\text{Bi}$ systems are similar [18], the authors concluded that the direct processes must have comparable strengths in both $^{9,11}\text{Be}$ nuclei and that the differences in binding energies and radii of the two Be isotopes do not play an important role, but rather collective excitations are more important. These conclusions are opposite to the ones reached with ^6He beams by different authors.

Since the quality of the above results is strongly limited by the beam quality itself, some years ago we proposed (experiment IS438) to make use of good quality post accelerated $^{10,11}\text{Be}$ beams at REX-ISOLDE to study elastic and direct reactions in collisions induced by ^{11}Be and its well bound core ^{10}Be on ^{64}Zn at the same center of mass energy $E_{\text{cm}}=24.5$ MeV. We used a detection system consisting of an array of Si-detector-telescopes each formed by a $40\ \mu\text{m}$ $50\times 50\ \text{mm}^2$, ΔE DSSSD detector (16×16 pixels) and a $1500\ \mu\text{m}$ single pad E detector. The detectors were placed very close to the target in order to have a large angular $10^\circ \leq \theta_{\text{lab}} \leq 150^\circ$ and solid angle coverage. A $550\ \mu\text{g}/\text{cm}^2$ and $1000\ \mu\text{g}/\text{cm}^2$ ^{64}Zn targets were used with ^{10}Be and ^{11}Be beams respectively. The target was tilted at 45° to facilitate the measurement in the angular region around 90° . The average beam intensity was 10^6 pps and 10^4 pps for ^{10}Be and ^{11}Be respectively.

The measured elastic scattering angular distributions are shown in figure 2. In the same figure we also show the elastic angular distribution for the $^9\text{Be}+^{64}\text{Zn}$ system measured at the Tandem of Laboratori Nazionali del Sud in Catania. The angular distribution for the ^{11}Be projectile shows suppressed elastic cross sections in the 'rainbow' region when compared with the ^{10}Be and ^9Be projectiles. This is a signature of long range interaction due to the diffuse structure of the neutron halo.

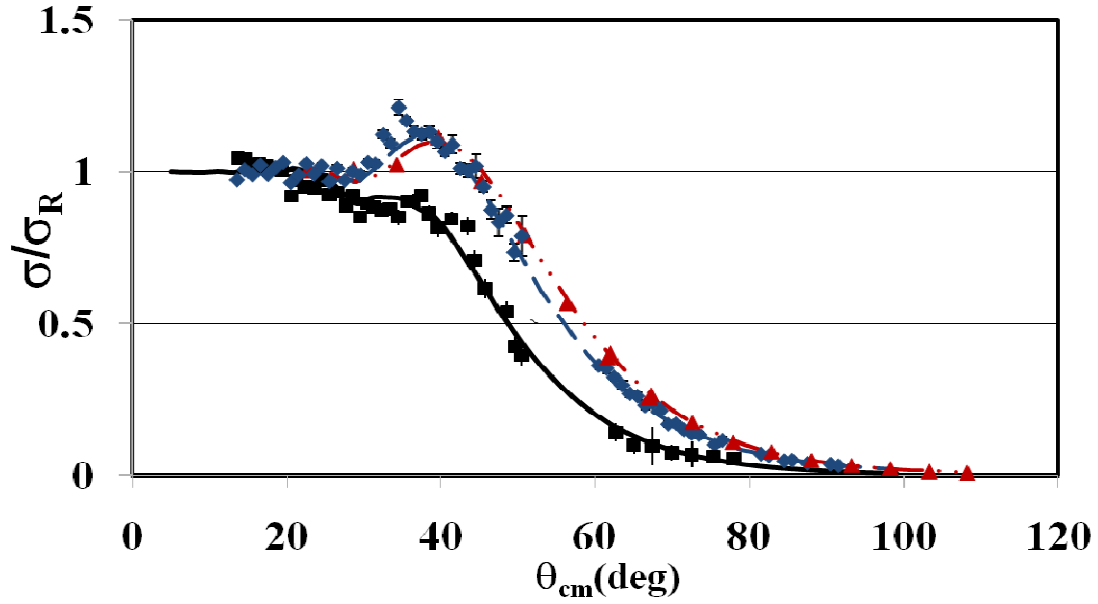


Figure 2. Angular distributions of the elastic scattering of ${}^9\text{Be}$ (triangles), ${}^{10}\text{Be}$ (diamonds) and ${}^{11}\text{Be}$ (squares) on ${}^{64}\text{Zn}$. The lines represent the OM calculations for ${}^9\text{Be}$ dot dashed, ${}^{10}\text{Be}$ (dashed) and ${}^{11}\text{Be}$ (full line).

The total reaction cross section σ_R is very sensitive to the shape of the elastic scattering angular distributions in this region. Performing optical model fits we obtained $\sigma_R \approx 2$ b for the ${}^{11}\text{Be}$ case and $\sigma_R \approx 1$ b for the ${}^9,{}^{10}\text{B}$ cases. For the ${}^{11}\text{Be}$ induced collision we also measured the angular distributions of ${}^{10}\text{Be}$ produced in transfer and breakup reactions giving a cross section for such direct mechanisms $\sigma_{\text{transfer/BU}} \approx 1$ b.

In summary the good quality of the post accelerated ${}^{10,11}\text{Be}$ beams at REX-Isolde, coupled with the large solid angle and elevate pixelization of the detection system used, allowed us to measure rather precise angular distributions for elastic scattering and direct reactions. It was measured a strong enhancement of the total reaction cross section due to a large yield for direct reaction processes. Moreover, large diffuseness of the imaginary part of the potential was needed to reproduce the elastic scattering angular distributions with Optical Model fits.

2. Proposed experiment

The dumping of the Coulomb-nuclear interference peak in the elastic scattering angular distribution, particularly evident in the ${}^{11}\text{Be}+{}^{64}\text{Zn}$ case, is originated by absorption occurring at large partial waves due to the halo structure. As mentioned above, the Optical Model analysis of the ${}^{11}\text{Be}+{}^{64}\text{Zn}$ elastic data showed that a very large surface diffuseness parameter ($a_{\text{si}}=3.5$ fm) is needed in order to reproduce the behavior of the cross-section in the region around the “rainbow”. This large diffuseness is related to the decay length of the neutron initial state wave function inside the halo nucleus [19]. The aim of the present experiment is to perform the measurement of a detailed elastic scattering angular distribution of the ${}^8\text{B}$ nucleus on a ${}^{64}\text{Zn}$ target in the angular range $15^\circ \leq \theta_{\text{cm}} \leq 140^\circ$ at

3 degree step, in order to investigate if similar effects are present in reactions induced by the p-halo ^8B nucleus at energies around the Coulomb barrier.

The only measured elastic scattering data using a p-halo nucleus, at energies around the barrier, are from E.F. Aguilera et al. [20]. They measured elastic scattering angular distributions of $^8\text{B}+^{58}\text{Ni}$, using the in-flight separated “cocktail” ^8B , ^7Be , ^6Li beam produced at the TwinSOL facility of Notre Dame at five different energies. In figure 3 it is shown, in linear scale, the elastic scattering angular distribution at $E_{\text{lab}}=25.3$ MeV from [20] (the data are taken from EXFOR). All other angular distributions in [20] have similar quality.

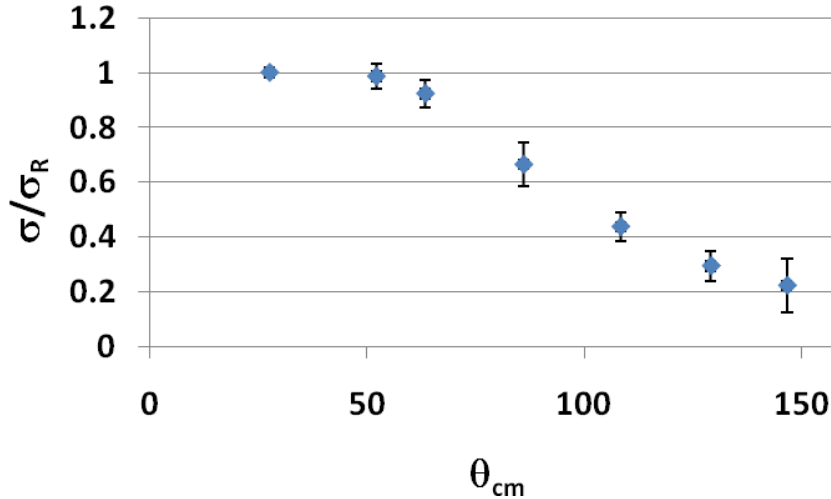


Figure3. Elastic scattering angular distribution of $^8\text{B}+^{58}\text{Ni}$ at $E_{\text{lab}}=25.3$ MeV [20].

As can be seen from the figure, the angular distribution was obtained with a limited number of measured angles. In particular, in the region around the “rainbow” only two or three points, depending on the beam energy, were measured. In [20], the angular range covered by each detector is not specified. As can be clearly seen from the comparison between fig.1 and fig. 2, only if precise measurements are performed one can observe structure effects on the elastic scattering angular distribution. Moreover, precise measurements are needed to extract reliably the total reaction cross-section from elastic scattering. In the $^{11}\text{Be}+^{64}\text{Zn}$ data, it was possible to observe the suppression of the elastic cross-section in the Coulomb-nuclear interference region, and the associated enhancement of the total reaction cross-section, thanks to the large number of measured angles and the small $\Delta\theta$ bin covered by each point.

Aim of the present proposal, in addition to the measurement of elastic scattering angular distribution and total reaction cross-section in $^8\text{B}+^{64}\text{Zn}$, is the measurement of the transfer/break-up angular distribution by measuring the emitted ^7Be particles.

3. Experimental set-up.

The proposed experimental set-up is similar to the one used for the $^{11}\text{Be}+^{64}\text{Zn}$ IS438 experiment, sketched in fig.4. The requested ^8B beam energy is 3.1 MeV/u, the maximum available energy at REX-Isolde.



Figure 4. Sketch of the experimental set-up used in the IS438 experiment.

A target of $1\text{mg}/\text{cm}^2$ will be surrounded by four Si detector telescopes and two $40\ \mu\text{m}$ DSSsS detectors (divided into 16+16 strips). These two last detectors will be placed at backward angles ($\theta_{\text{cm}} > 110^\circ$). Each telescope will be composed by a $20\ \mu\text{m}$ ΔE Si strip detector ($50 \times 50\ \text{mm}^2$ divided into 16 strips) and a 500 or $1000\ \mu\text{m}$ residual energy DSSsD detector ($50 \times 50\ \text{mm}^2$ divided into 16+16 strips). With this set-up the angular range $15^\circ \leq \theta_{\text{cm}} \leq 140^\circ$ can be covered. With the proposed detection system we aim to measure the elastic scattering angular distribution at 3 degree steps. We will be able to charge identify the scattered ^8B particles up to $\theta_{\text{cm}} \approx 110^\circ$. At very backward angles the energy of the scattered ^8B particles will not be sufficient to punch through the $20\ \mu\text{m}$ ΔE detector. We expect that at backward angles the only particles reaching the detectors are H, He and B. Although at $\theta_{\text{cm}} > 110^\circ$ we will not be able to identify neither in mass nor in charge, using $40\ \mu\text{m}$ detectors we expect to obtain a clean B spectrum in the region from $13\ \text{MeV}$ to $16\ \text{MeV}$, where the elastic scattering is expected to contribute. The maximum energy deposited by H and He in $40\ \mu\text{m}$ Si is, in fact, $1.8\ \text{MeV}$ and $7\ \text{MeV}$ respectively. The kinematics for $^8\text{B} + ^{64}\text{Zn}$ elastic scattering at $E_{\text{lab}} = 24.8\ \text{MeV}$ is shown in fig. 5, the energy loss in half the target is considered. The target will be tilted at 45° with respect to the beam axis in order to allow measuring also at angles around 90° .

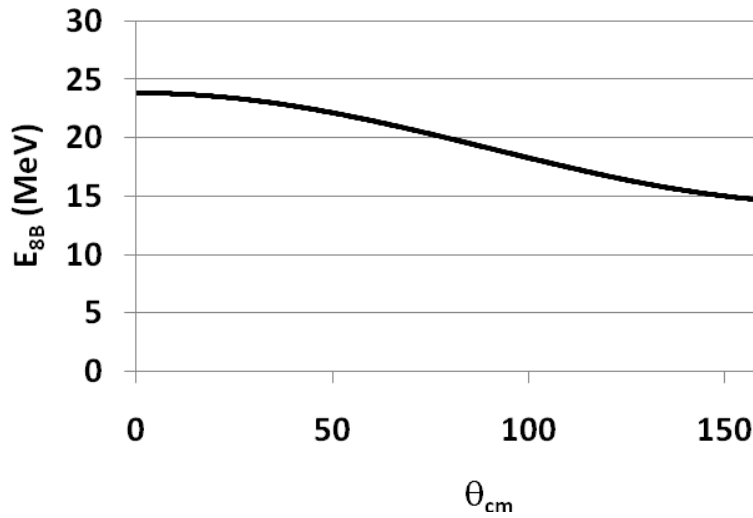


Figure 5. Kinematics of ^8B scattered by a ^{64}Zn target at $E_{\text{lab}}=23.9$ MeV.

4. Beam time request.

For the requested beam time we assumed an average ^8B intensity of 5×10^3 pps. As above mentioned we aim at measuring the angular distribution at 3° steps at least in the angular region up to 110° . At backward angles a 5° step will be used. With the proposed geometry we will be able to measure in 21 shifts the angular distribution in the range $15^\circ \leq \theta_{cm} \leq 60^\circ$ with a statistical error from 0.2% to 4%. The statistical error at the largest angles will be comparable with the measurement of [20].

Five additional shifts of stable beam (^{12}C) are requested to set-up the electronics and for the angle and solid angle determination of the detector pixels, using Rutherford scattering on a Au target.

We are not asking additional beam time for beam development, we were informed that this beam time is allocated within the target and ion source development (TISD) if the proposal is approved.

Four more shifts are requested for post-acceleration and beam contamination tests to verify the beam intensity and purity after the post acceleration.

6. Conclusions

In conclusion, we would like to point out that a post accelerated ^8B beam is not available in any other ISOL facility worldwide. To have such a beam at ISOLDE will certainly be of interest of many other groups. With the present proposal, interesting information about ^8B structure effects on reaction mechanisms can be obtained even if a very low intensity ^8B beam will be obtained. Of course, if the beam intensity will be higher, more information can be obtained even in the present proposed experiment. For example from the ^7Be -p coincidence measurements one can obtain information on the separate contribution of transfer and break-up onto the direct processes cross-section.

If the present proposal will be approved, we aim to measure, as comparison, the elastic scattering angular distribution for the corresponding stable isotopes $^{10,11}\text{B}$ onto the same ^{64}Zn target at the same E_{cm} . These experiments will be performed at the Laboratori Nazionali del Sud in Catania.

References

- 1) N.Keeley et al. Prog. Part. Nucl. Phys. 63, 396 (2009)
- 2) A. Di Pietro et al. Phys.Rev. C69, 044613 (2004)
- 3) A.M. Sanchez-Benitez et al. Nucl. Phys. A803, 30 (2008)
- 4) S.Frike et al. Nucl.Phys. A500, 399 (1989)
- 5) E.F.Aguilera et al. Phys Rev. C63, 061603 (2001)
- 6) R.Raabe et al. Nature 431, 823 (2004)
- 7) J.J. Kolata et al. Phys Rev. C75, 031302 (2007) and references therein
- 8) A. Chatterjee et al. Phys. Rev. Lett. 101, 032701 (2008)
- 9) J.J.Kolata et al. Phys Rev. Lett. 81, 4580 (1998)
- 10) Yu.E. Penionzhkevich et al. Eur. Phys. J. A 31, 185 (2007)
- 11) O. Kakuee et al. Nucl. Phys. A 728, 339 (2003)
- 12) Y. Kucuk et al. Phys. Rev. C79, 067601 (2009)
- 13) A. Moro et al. Phys. Rev. C75, 064607 (2007)
- 14) T. Matsumoto et al. Phys. Rev. C73, 051602R (2006)
- 15) M. Rodríguez-Gallardo et al. Phys. Rev. C77, 064609 (2008)
- 16) N.Keeley et al. Prog. Part. Nucl. Phys. 59, 579 (2007)
- 17) M.Mazzocco et al. Eur. Phys. Jour. S.T. 150, 37 (2007)
- 18) C.Signorini et al. Nucl. Phys. A 735, 329 (2004)
- 19) A. Bonaccorso and F. Carstoiu, Nucl. Phys. A 706, 322 (2002).
- 20) E.F. Aguleira et al. Phys. Rev. C 79, 021601(R) (2009)